31st Annual International Conference of the IEEE EMBS
Minneapolis, Minnesota, USA, September 2-6, 2009

Mechanisms Determining Safety and Performance of Brain Stimulating Electrodes

Dana Lynn Andre, *Student Member, IEEE*, Balaji Shanmugasundaram, Jonathan Mason, Corina Drapaca, *Member, IEEE* and Bruce J. Gluckman, *Member, IEEE*

Abstract— **Electrical current is widely used to interact with or stimulate neural systems. Current transduction from device to tissue is mediated at the electrode-tissue interface by capacitive charge and electrochemistry. This charge-passing-capacity is frequency dependent. While safety parameters have been established for high-frequencies, safety has not been fully determined for novel materials and pulse frequencies significantly lower than 100 Hz. We are explicitly interested in safety parameters and performance of charge passing at low frequencies (<<100 Hz) for neural systems. We present a visual study of pH during charge passing for electrodeposited iridium oxide electrodes. Clear reaction-diffusion waves are observed that extend many hundreds of micrometers from the electrode surface.**

I. Introduction

ELECTRICAL current is widely used to interact with or stimulate neural systems. Both high- and low-frequency simulation can be used to modulate neural activity.

High-amplitude, high-frequency content (<<1 ms) pulse stimulation can cause action potentials to occur and thereby alter natural neuronal behaviors. In contrast, low-amplitude polarizing low-frequency (>>20 ms) electrical fields (PLEF) have a subthreshold effect, meaning they do not induce action potentials. PLEF reorganizes internal charge, altering the neuron's response to its intrinsic input by locally hyperpolarizing or depolarizing the soma. This modulation is proportional to the amplitude and sign of applied field (Fig. 1). We have demonstrated this ability to modulate seizure activity in vitro [1].

Manuscript received April 7, 2009. This work was supported in part by the Pennsylvania Dept of Community & Economic Development Keystone Innovation Grant.

D. L. Andre is a graduate student with the Department of Engineering Science and Mechanics at the Pennsylvania State University, University Park, PA 16802 USA (814-865-2481; fax: 814-550-2150; e-mail: DanaAndre@psu.edu).

B. Shanmugasundaram is a graduate student with the Department of Engineering Science and Mechanics at the Pennsylvania State University, University Park, PA 16802 USA (e-mail: s.balaji@psu.edu).

J. Mason is a lecturer with the Department of Engineering at the University of Waikato, Hamilton, New Zealand (e-mail: jmason @waikato.ac.nz).

C. Drapaca is an assistant professor with the Department of Engineering Science and Mechanics at the Pennsylvania State University, University Park, PA 16802 USA (e-mail: csd12@psu.edu).

B. J. Gluckman is an associate professor with the Department of Engineering Science and Mechanics at the Pennsylvania State University, University Park, PA 16802 USA and also with the Department of Neurosurgery at the Hershey Medical Center, Hershey, PA 17033 USA (e-mail: BruceGluckman@psu.edu).

When instrumented correctly, PLEF can be applied simultaneous to neural recording with minimal recording artifact, thereby allowing the implementation of continuous feedback control. PLEF has been successfully used for the suppression of epileptiform activity in vitro in rat hippocampal slices when applied as a negative feedback control [2].

We have now developed a prototype system for applying PLEF in chronically implanted animals, and demonstrated the ability to interact with spontaneous seizure activity [3], [4].

For purposes such as PLEF, electric fields are generated by electrodes in the brain. Brain tissue is conductive, so the fields are accompanied by electrical current that is passed between the electrodes. Charge transfer is mediated by both Faradaic reactions and capacitive charge at the electrode-tissue interface. The duration and amplitude of applied fields are therefore limited at least in part by the safety limitations of charge passing at the electrode surfaces.

Safety parameters for high-frequency stimulation have been established by McCreery et al, Yuen et al, and others [5], [6]. When examining charge density versus total charge, it was found that high levels of charge can only be passed at low charge densities, while low levels of charge can be passed at a broad range of charge-densities [7]. Unfortunately, these empirical guidelines do not apply to low-frequency content stimulation (<<100 Hz).

Improperly selected parameters can cause severe damage due to phenomena shown in Fig. 2. Here, 125 μm polyimide insulated stainless steel electrodes passed a 1 Hz 50 μA sinusoidal current into a 0.3% (weight/volume) agarose and 0.9% saline solution. We see bubble formation indicative of hydrolysis. Surprisingly, these parameters have been used as a method of seizure prevention in vivo in rats [8].

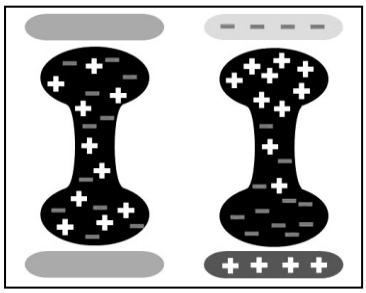

Fig. 1. Charge distribution in a neuron with and without an external electric field. The neuron's chance of firing increases or decreases based on its polarization.

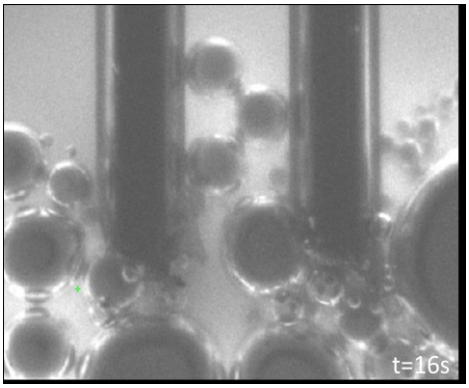

Fig. 2. Two 125µm polyimide insulated stainless steel electrodes stimulating with a 1Hz, 50µA square-wave. Such gas bubbles are probably harmful.

In order to pass higher amounts of charge without causing hydrolysis of the tissue, we need biocompatible electrodes with higher charge passing capacity. Capacitive charge transfer can be improved by increasing surface area at the nanoscale level. On the other hand, reversible Faradaic reactions are capable of passing more charge without producing harmful products. Iridium oxide is one such material that can pass higher charge by simply changing oxidation levels through the following reaction (1) [7].

$$2IrO_2 + 2H^+ + 2e^- \leftrightarrow Ir_2O_3 + H_2O \quad (1)$$

We utilize electrodeposited iridium oxide films (EIROF) in our chronic implants to increase charge passing capacity [3,4]. But, the performance of these electrodes, in terms of charge passing capacity, is far lower in vivo than in vitro, and decreases as a function of application frequency, as shown in Fig. 3.

Cogan et al. have recently shown that the charge passing capacity of iridium oxide electrodes depends largely on the buffering capacity of the test electrolyte [7]. As shown, the charge transfer reaction in iridium oxide involves the insertion or ejection of H^+or OH^- ions which will lead to

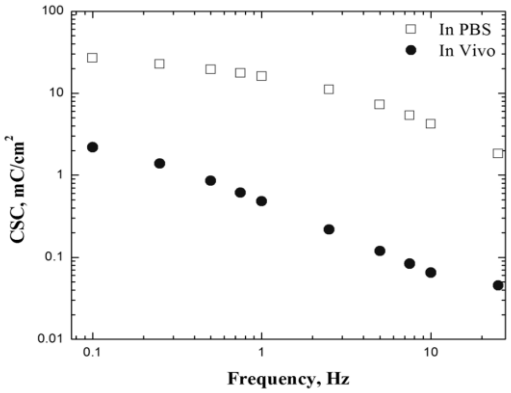

Fig. 3. Charge storage capacity of EIROF coated stainless steel electrodes in vitro (phosphate buffered saline) and chronic in vivo (after one week of implantation). Note that performance decreases in vivo.

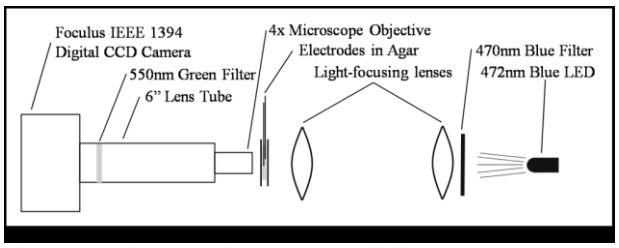

Fig. 4. Optical setup used to measure pH field.

local changes in pH around the electrodes. Thus, the decreased performance of EIROF in chronic in vivo conditions as shown in Fig. 3 could be a result of slower mass transport and poor buffering capacity of the brain tissue.

Our objective is to elucidate the dependencies of mass transport and the spatial distribution of buffering agents on the pH changes around the electrode. We have implemented a pH field visualization technique based on fluorescent imaging with pH-sensitive dye. This knowledge will further optimize the stimulation parameters and to develop better electrode-tissue interfaces and materials.

II. Materials and Methods

A. Test Medium

To observe pH changes, we test electrodes in a pH-sensitive agarose gel containing fluorescein 0.08% (weight/volume), agarose 0.3% and either physiological saline or artificial cerebral spinal fluid. Fluorescein is a commonly used dye and is pH-dependent. More specifically, it is a complex fluorophore that exists in any of four prototropic forms (cation, neutral, monoanion, dianion) in a pH range 1-10. As pH decreases, H^+ ions become more plentiful, binding to the fluorescein and changing its prototropy. Lower proton levels correlate to higher fluorescent emission efficiencies [10]. In our imaging, this means that brighter areas have higher pH levels and darker areas have lower levels.

B. Experimental Setup

The experimental setup contains a 472 nm blue LED illuminator, 470 nm blue filter and two lenses (Fig. 4). The image is magnified by an Olympus PlanAchro 4x microscope objective before passing through a 550 nm green filter to a black and white Foculus IEEE 1394 Digital CCD camera. The blue filter eliminates fluorescence produced in the LED casing while the green filter limits collection at the camera to only the fluorescent light from the fluorescein. The entire setup is enclosed in a dark box. Standard potentiostat and galvanostat circuits were used for electrochemical measurements and electrical stimulations [11]. Signal generation, video recordings and data acquisition were performed using custom designed LabView VIs interfaced by NI PCI 6221 boards and an IEEE1394 interface.

C. Electrodes

The microelectrodes were made of polyimide-coated

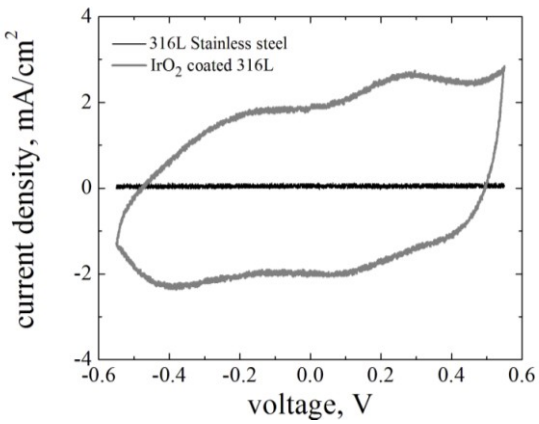

Fig. 5. CV comparison of an uncoated and EIROF coated 250 µm diameter 316L stainless steel microwire electrodes.

250 µm diameter 316L stainless steel microwires. Iridium oxide electrodeposition was carried out in a electrolyte consisting of 4mM $IrCl_4$ in 40mM oxalic acid buffered to 10.4 pH using 3M K_2CO_3 [12]. Cyclic voltammetry (CV) measurements were obtained in phosphate buffered saline solutions at 50 mV/s scan rate between limits of -0.6 and +0.6 V vs SCE reference (Fig. 3). Cathodic charge storage capacity (CSC_c) is measured as the area under the cathodic region of the cyclic voltammogram. The electrodes were stimulated with 1Hz square waveform currents of different amplitudes. The animal studies in Fig. 3 were performed in accordance with a protocol approved by the Pennsylvania State University Institutional Animal Care and Use Committee.

III. Results

The CVs of typical uncoated and EIROF coated 316L stainless steels are shown in Fig. 5. About two orders of magnitude improvement in CSC is achieved for EIROF (46 mC/cm^2) as compared to the uncoated 316L stainless steel electrodes (0.05 mC/cm^2) at 50 mV/s scan rate, which is reflected in the CV by the increased enclosed area of the EIROF CV (grey line) vs. that of the bare electrode (black line), which has no discernable open area at this scale.

The CV is performed with a voltage-controlled triangle waveform with a frequency of about 0.02 mHz. As waveform frequency is increased (0.1-25 Hz) the charge storage capacity of the EIROF electrodes decreases as shown in Fig. 3. A significant decrease in CSC occurs at all frequency ranges (0.1-25 Hz) when the electrodes are shifted

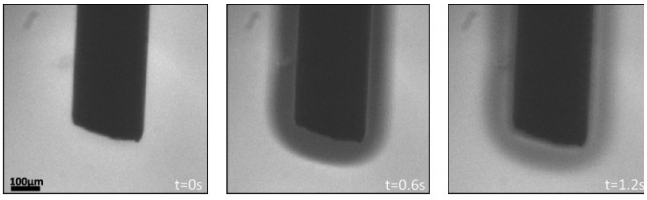

Fig. 6. pH variations surrounding a 250 µm EIROF coated stainless steel electrode passing a square wave of current (1 Hz, 500µA). The first image is baseline, with no current passing. Decreases in intensity correspond to increases in acidity.

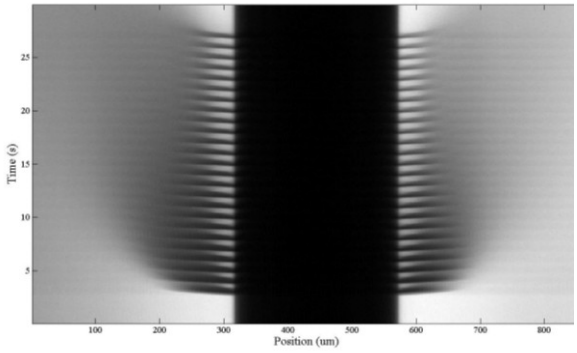

Fig. 7. Space-time dependence of pH for same data as Fig 6. Each horizontal line in the image corresponds to the intensity of the image as a function of position perpendicular to its axis, averaged over approximately 1 mm of one diameter of the electrode. The observed stripes show propagation of pH variations into the surrounding agar.

from phosphate buffered saline to the brain tissue environment.

An example of the pH field variation during low-frequency (1 Hz) stimulation is shown in Figs. 6 and 7, under current controlled charge passing conditions with half cell potentials well within the water window (beyond which water hydrolyzes) for these electrodes. Acidic changes (dark) initiate at the electrode surface and propagate outward hundreds of micrometers into the surrounding medium (Fig. 6).

Increasing current caused pH changes to extend farther into the test medium. Changes in pH were asymmetrical, most likely due to the arrangement of the two electrodes used (Fig. 7). Fluctuations were most drastic closest to the electrode and smoother farther away (Fig. 8).

In saline, bubble formation occurred at 900 µA in the EIROF electrodes, versus 100 µA in the uncoated stainless steel.

The observations of space-time varying pH variations were observed for a broad range of currents and waveforms for EIROF electrodes. These pH variations are consistent with reaction-diffusion waves driven by the electrically driven H^+ flux at the electrode surfaces. Reaction diffusion waves are the result of processes in which local reactions couple spatially through diffusion processes. We can, and in future work will, therefore computationally model these experimentally observed changes in pH. The Nernst

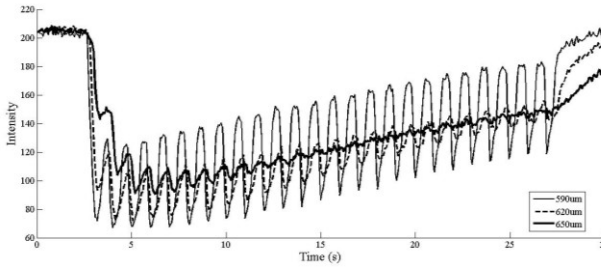

Fig. 8. pH variations as function of time for specific distances from the electrode for same data as Figs. 6,7. Different lines correspond to horizontal positions in Fig. 7.

equation and Fick's Law are combined to merge the effects of the electrical field with the chemical reactions occurring (2, 3, 4).

$$\frac{\partial[H^+]}{\partial t} = D\left(\frac{-d^2[H^+]}{dx^2} + \frac{eE}{K_B T}[H^+]\right) - k_1[H^+][OH^-] + k_2 \quad (2)$$

$$\frac{\partial[OH^-]}{\partial t} = D\left(\frac{-d^2[OH^-]}{dx^2} - \frac{eE}{K_B T}[OH^-]\right) - k_1[H^+][OH^-] + k_2 \quad (3)$$

$$H_2O \underset{k_1}{\overset{k_2}{\rightleftharpoons}} H^+ + OH^- \quad (4)$$

In these equations, k_1 and k_2 are rate constants for the dissociation of water (4). The diffusivity coefficient, D, represents the rate at which relevant species diffuse through the medium. These equations would be augmented by the concentration dynamics of other chemical species involved in supplementary buffering mechanisms. Collectively, (2-4) model how the included parameters affect the pH and CSC.

IV. Concluding Remarks

We have developed an experimental system for measuring pH fields around the electrode during charge passing. We observe significant reaction-diffusion waves by visualizing $[H^+]$ using pH-sensitive fluorescence. We know that pH variations are inherently bad for the brain and observe that they also limit the charge-passing capabilities of the electrode. Our methodology can be used to test new thin-film coatings. Additionally, it can be used in live tissue to understand buffering and diffusion in the brain.

References

[1] B. J. Gluckman, E. J. Neel, T.I. Netoff, W. L. Ditto, M. L. Spano, S. J. Schiff. "Electric field suppression of epileptiform activity in hippocampal slices," *J Neurophysiol*., vol. 76, pp. 4202-4205, Dec. 1996.

[2] B. J. Gluckman, H. Nguyen, S. L. Weinstein, S. J. Schiff. "Adaptive Field Control of Epileptic Seizures," *J Neurosci*., vol. 21, pp. 590-600, Jan. 2001.

[3] S. Sunderam, N. Chernyy, J. Mason, N. Peixoto, S. L. Weinstein, S. J. Schiff, B. J. Gluckman. "Seizure Modulation with Applied Electric Fields in Chronically Implanted Animals," in *2006 Proc. 28th IEEE EMBS Annual Intl. Conf.*, pp. 1612-15.

[4] S. Sunderam, N. Chernyy, H. Peixoto, J. P. Mason, S. L. Weinstein, S. J. Schiff, B. J. Gluckman. "Seizure entrainment with polarizing low frequency electric fields in a chronic animal epilepsy model," *J Neural Eng*., to be published.

[5] D. B. McCreery, W. F. Agnew, T. G. Yuen, L. Bullara. "Charge density and charge per phase as cofactors in neural injury induced by electrical stimulation," *IEEE Trans. Biomed. Eng.*, vol. 37, pp. 996-1001, Oct. 1990.

[6] T. G. Yuen, W. F. Agnes, L. A. Bullara, S. Jacques, D. B. McCreery. "Histological evaluation of neural damage from electrical stimulation: considerations for the selection of parameters for clinical application," *Neurosurgery*, vol. 9, pp. 292-299, Sep. 1981.

[7] D. R. Merrill, M. Bikson, and J. G. R. Jefferys. "Electrical stimulation of excitable tissue: design of efficacious and safe protocols," *J Neurosci. Methods*, vol. 141, pp. 171-198, Feb. 2005.

[8] J. H. Goodman, R. E. Berger, and T. K. Tcheng. "Preemptive low-frequency stimulation decreases the incidence of amygdala-kindled seizures," *Epilepsia*, vol. 46, pp. 1-7, Jan. 2005.

[9] S. F. Cogan, P. R. Troyk, J. Ehrlich, C. M. Gasbarro, T. D. Plante. "The influence of electrolyte composition on the in vitro charge-injection limits of activated iridium oxide (AIROF) stimulation electrodes," *J Neural Eng.*, vol. 4, pp79-86, Mar. 2008.

[10] J. M. Alvarez-Pez, L. Ballesteros, E. Talavera, J. Yguerabide.,"Fluorescein Excited-State Proton Exchange Reactions: Nanosecond Emission Kinetics and Correlation with Steady-State Fluorescence Intensity," *J. Phys Chem. A*, vol. 105, pp. 6320-6332, Apr. 2001.

[11] A. J. Bard, L. R. Faulkner, *Electrochemical Methods: Fundamentals and Applications*. New York: Wiley, 2000, pp. 632-658.

[12] R. D. Meyer, S. F. Cogan, T. H. Nguyen, R. D. Rauh. "Electrodeposited iridium oxide for neural stimulation and recording electrodes," *IEEE Trans Neural Syst Rehabil Eng.*, vol. 9, pp. 2-11, Mar. 2001.